

# PMN J1632–0033: A strong gravitational lens candidate

Joshua N. Winn<sup>1,2</sup>, Jacqueline N. Hewitt<sup>1</sup>, James E.J. Lovell<sup>3</sup>, Nicholas D. Morgan<sup>1</sup>, Alok R. Patnaik<sup>4</sup>, Bart Pindor<sup>5</sup>, Paul L. Schechter<sup>1,2</sup>, Robert A. Schommer<sup>6</sup>

## ABSTRACT

We report the discovery of a double radio source that is probably a two-image gravitational lens. The object J1632–0033 is composed of two compact, flat-spectrum components with separation  $1''.47$  and flux density ratio 12.4. The spectral indices of the components are the same within 0.05, as determined by measurements ranging from 1.4 GHz to 43 GHz using the VLA, ATCA, MERLIN and VLBA. The optical counterpart is double, with roughly the same separation and position angle as the radio double. An optical spectrum of the bright component, obtained with the first Magellan telescope, reveals quasar emission lines at redshift 3.42. Although J1632–0033 could be a binary quasar, the small separation and similarity of radio continuum spectra of the components suggest that they are lensed images of a single quasar.

*Subject headings:* gravitational lensing, quasars: individual (J1632–0033)

## 1. Introduction

When a galaxy happens to lie along nearly the same line of sight as a more distant object, gravitational lensing by the galaxy may cause multiple images of the background object to appear in the sky. These cases of “strong” lensing (as opposed to “weak” lensing, in which images of background objects are distorted but not multiply imaged) can be used to measure the masses (e.g., Kochanek 1995) and extinction laws (e.g., Falco et al. 1999) of distant galaxies, and to determine the Hubble constant (Refsdal 1964) and cosmological constant (Turner 1990; Fukugita, Futamase & Kasai 1990), among other applications (for reviews, see Narayan 1998; Blandford & Narayan 1992).

---

<sup>1</sup>Department of Physics, Massachusetts Institute of Technology, Cambridge, MA 02139

<sup>2</sup>Visiting Astronomer, Cerro Tololo Inter-American Observatory, National Optical Astronomy Observatories

<sup>3</sup>Australia Telescope National Facility, CSIRO, PO Box 76, Epping, NSW 1710, Australia

<sup>4</sup>Max-Planck-Institut für Radioastronomie, Auf dem Hügel 69, 53121 Bonn, Germany

<sup>5</sup>Princeton University Observatory, Peyton Hall, Princeton, NJ 08544-1001

<sup>6</sup>Cerro Tololo Inter-American Observatory, National Optical Astronomy Observatories, Casilla 603, La Serena, Chile

We have been conducting a survey for new lenses to be used in these applications. Our search strategy relies on the fact that the great majority ( $\sim 95\%$ ) of flat-spectrum radio sources are quasars which appear as point sources in VLA images with  $0''.3$  resolution. Those few sources exhibiting multiple compact components with separations ranging from  $0''.4$  to  $5''$  (a typical angular scale that is set by the mass of  $L_*$  galaxies at medium redshifts) are good lens candidates. Ours is the latest in a series of VLA-based surveys for gravitational lenses (Lawrence et al. 1986; King et al. 1998; Browne & Myers 2000), and is the first to explore the southern sky accessible to the VLA ( $0^\circ > \delta > -40^\circ$ ).

Our initial sample of 4097 flat-spectrum radio sources was generated by cross-correlating the PMN (4.85 GHz; Griffith & Wright 1993) and NVSS (1.4 GHz; Condon et al. 1998) catalogs. To date, we have created 8.5 GHz images of 3850 (94%) of these objects based on new and archival data from the VLA in its A-configuration. We identified those objects with multiple compact components as gravitational lens candidates.

Most of the follow-up effort is devoted to the candidates with two components, because there is a large population of contaminants to contend with: core-jet sources. In these sources, although both components may appear compact with  $0''.3$  resolution, typically one component (the core) is flat-spectrum and compact on milliarcsecond scales, and the other component (a hot spot in a jet or lobe) is steep-spectrum and extended on milliarcsecond scales. These objects constitute over 90% of our two-component lens candidates. They are rejected by radio follow-up observations with higher spatial resolution, and at multiple frequencies.

The object presented in this paper, J1632–0033, has passed these radio filters. It is a double with separation  $1''.47$ . The flux density ratio of these components is roughly the same at every radio frequency for which we have measurements, from 1.4 GHz to 43 GHz. Both components are compact on milliarcsecond scales.

We believe this is strong evidence that the components of J1632–0033 are multiple images of a single background radio source. However, it is possible that they are a physically associated pair of quasars that happen to have the same radio continuum spectra. A definitive way to discriminate between these hypotheses is to search for a foreground galaxy in a high-resolution optical image. Such was the case for the first two lenses discovered in our survey, J1838–3427 (Winn et al. 2000) and J2004–1349 (Winn et al. 2001a). The optical images presented in this paper are not sufficiently deep to test for the presence of a lens galaxy, and therefore cannot rule out the binary quasar hypothesis—although they do confirm that the optical counterpart is double with roughly the same separation and position angle as the radio double.

Section 2 presents the radio observations. Section 3 presents optical data, both from direct images (§ 3.1) and spectroscopy (§ 3.2). Finally, § 4 discusses the relative likelihood of four hypotheses to account for the observations, including the gravitational lensing and binary quasar hypotheses, and describes prospects for future observations.

## 2. Radio observations

Table 1 lists the radio observations with the VLA, VLBA<sup>7</sup>, MERLIN<sup>8</sup>, and ATCA<sup>9</sup> in chronological order. The first 3 entries represent archival VLA data that we obtained and reduced; the remaining 9 are observations that we conducted after identifying J1632–0033 as a gravitational lens candidate. The coordinates of J1632–0033 are given in the comment beneath Table 1.

In all the images, there are two components. We refer to the northwest (brighter) component as A, and the southeast (dimmer) component as B. The components are compact in all the images except the VLBA image, in which component A is partially resolved. Figure 1 displays a representative VLA image of the system, as well as higher-resolution VLBA images of each component.

### 2.1. Data reduction and analysis

The details of the data reduction and analysis are as follows:

**VLA.** The VLA data were calibrated with standard routines in the software package AIPS. For the first three VLA observations (1984–1999), radio source 3C286 was used to set the absolute flux density scale, using the procedures recommended in the VLA Calibrator Manual. For the VLA observations in 2000, the source J2355+4950 was used instead; this compact source is monitored monthly by G. Taylor and S. Myers of NRAO, and has been found to have a stable flux density. The assumed flux densities of J2355+4950 were 2.306 Jy (1.4 GHz), 0.602 Jy (15 GHz), 0.473 Jy (22.5 GHz), and 0.284 Jy (43 GHz). We applied gain-elevation corrections for data at 15 GHz and higher frequencies based on gain curves prepared by S. Myers.

Imaging and analysis were performed with the software package Difmap. We fitted a surface-brightness model consisting of 2 circular Gaussian components to the visibility function, and used this model to perform phase-only self-calibration with a solution interval of 30 seconds. This process, model-fitting and self-calibration, was repeated (typically 3 times) until the model converged. For the 1.4 GHz data, which had the lowest spatial resolution, we fixed the relative separation and orientation of the model components at the values obtained from the VLBA data.

**MERLIN.** Calibration of the MERLIN data was performed at Jodrell Bank using both standard MERLIN software and AIPS. The absolute flux scale was set by observing 3C286 and assuming

---

<sup>7</sup>The Very Large Array (VLA) and Very Long Baseline Array (VLBA) are operated by the National Radio Astronomy Observatory, a facility of the National Science Foundation operated under cooperative agreement by Associated Universities, Inc.

<sup>8</sup>The Multi-Element Radio Linked Interferometry Network (MERLIN) is a UK national facility operated by the University of Manchester on behalf of SERC.

<sup>9</sup>The Australia Telescope Compact Array (ATCA) is part of the Australia Telescope which is funded by the Commonwealth of Australia for operation as a National Facility managed by CSIRO.

a flux density of 7.38 Jy on the shortest baseline. Imaging and analysis were performed with Difmap in the same manner as for the VLA data.

**ATCA.** The ATCA data were calibrated using the software package MIRIAD. The absolute flux density scale of the ATCA data was set by observations of PKS B1934–638. The imaging and analysis steps were the same as for the VLA and MERLIN data. As with the 1.4 GHz VLA data, the relative separation of the two model components was kept fixed at the values derived from the VLBA data, in order to improve the accuracy with which we could extract separate flux densities for A and B.

**VLBA.** For the VLBA observation, the total observing bandwidth was divided into 4 intermediate frequency bands, each of which was subdivided into  $16 \times 0.5$  MHz channels. Fringe-fitting, calibration, and imaging of the VLBA data were all performed with AIPS. After fringe-fitting, we reduced the data volume by averaging in time into 6-second bins and in frequency into 1 MHz bins. These values were chosen to reduce the data volume as much as possible while keeping the amount of bandwidth smearing and time-average smearing below 1% over the required field of view.

For over 90% of our two-component lens candidates, only one component was detected by the VLBA, and the other component (presumably a jet or lobe) was resolved out. In this case, both components were obvious in the “dirty” image (prior to deconvolution). We employed the multiple-field implementation of the CLEAN algorithm, with a  $180 \text{ mas} \times 180 \text{ mas}$  field centered on each component. The model developed by the CLEAN algorithm was used to self-calibrate the antenna phases with a solution interval of 30 seconds. We iterated this process 5 times before arriving at the final model. The images based on this model, with uniform weighting and an elliptical Gaussian restoring beam, are displayed in Figure 1.

## 2.2. Total flux and flux density ratio

The flux densities of A and B are reported in Table 1 for each observation, along with the RMS noise level and an estimate of the uncertainty in the absolute flux scale. These numbers were used to generate the two plots presented in Figure 2.

The top panel of Figure 2 is a logarithmic plot of the total flux density of both components as a function of radio frequency. This reveals that J1632–0033 has a fairly flat radio spectrum. From 5 GHz to 22.5 GHz, the data that were all taken in the year 2000 are a good match to the power law  $S_\nu \propto \nu^{-0.3}$ . At 8.5 GHz, there is evidence for variability at the 5–10% level on a time scale of years. (The discrepancies between the 5 GHz measurements are more difficult to interpret, because the VLBA and MERLIN probe much smaller spatial scales than the other 5 GHz observations.)

The bottom panel is a logarithmic plot of the flux density ratio as a function of radio frequency. If the components had different radio continuum spectra, as was the case for the majority of our two-component lens candidates, one would observe this ratio to vary significantly with frequency.

Instead, it is apparent that the flux density ratio varies little, if at all, between 1.4 GHz and 43 GHz. The mean flux density ratio is 12.4. Because gravitational lensing is achromatic, gravitationally lensed images should have similar radio continuum spectra. The near-constancy of the A/B flux density ratio is therefore a natural consequence of the lensing hypothesis.

Assuming that component A obeys  $S_\nu(A) \propto \nu^\alpha$ , and likewise  $S_\nu(B) \propto \nu^\beta$ , one would expect the slope of the second plot of Figure 2 to be  $\alpha - \beta$ . A linear least-squares analysis of the data gives  $\alpha - \beta = 0.018 \pm 0.011$ , favoring a steeper spectrum for component B.

Even if this small discrepancy between spectral indices is real, it is consistent with the lensing hypothesis; due to the time delay, the instantaneous flux density ratio will vary if the background source is variable. Since J1632–0033 is evidently variable at the 5–10% level at 8.5 GHz, and is likely to be even more variable at the lowest and highest frequencies of our measurements, the important point is that the flux density ratios agree within 15% across a factor of 30 in radio frequency. In our subsequent discussion we assume  $\alpha - \beta < 0.05$ .

### 3. Optical observations

#### 3.1. Optical images

If J1632–0033 is a binary quasar, one would expect the optical counterpart to be double, if the image had a high enough resolution and signal-to-noise ratio. The optical flux ratio of the quasars would not necessarily be the same as the radio flux ratio. Likewise, the optical colors of the quasars would not necessarily be identical, although they would be similar because the quasars are at the same redshift.

In the case of a lens, the optical counterpart would also be double. In the simplest scenario, the optical flux ratio would equal the radio flux ratio, and the optical colors would be identical, because lensing is achromatic. However, the lensing galaxy complicates the situation by contributing its own light and possibly by altering the quasar light due to dust extinction, reddening, and microlensing. The detection of a diffuse source of light between a pair of quasars is among the best possible evidence that it is a pair of lensed images rather than a binary quasar.

On 2000 July 25 we obtained optical images of J1632–0033 with the Blanco 4-meter telescope at CTIO<sup>10</sup>. We used the Mosaic II camera, which has eight  $2048 \times 2048$  CCDs that are individually amplified and read out in pairs. We centered the target in chip #2. The night was photometric. After extracting the images from chip #2, we corrected them for cross-talk from the paired amplifier, bias-subtracted and flat-fielded them with standard IRAF procedures, and defringed the *I*-band

---

<sup>10</sup>Cerro Tololo Inter-American Observatory (CTIO) is operated by the Association of Universities for Research in Astronomy Inc., under a cooperative agreement with the National Science Foundation as part of the National Optical Astronomy Observatories.

images using a fringe template kindly supplied by R.C. Dohm-Palmer.

We measured the total instrumental magnitude of J1632–0033 in each image using a synthetic aperture of diameter  $7''$ . The zero point was determined by measuring the instrumental magnitude of the standard star SA110–361 (Landolt 1992) within an aperture of diameter  $14''$ . We adopted “typical” CTIO extinction coefficients of  $k_I = 0.06$ ,  $k_R = 0.11$ ,  $k_V = 0.15$ , and  $k_B = 0.28$  (Landolt 1992). Table 2 reports the filter, exposure time, airmass, and seeing of each observation, along with the with the calibrated magnitudes of J1632–0033. The top panel of Figure 3 shows the  $5' \times 5'$  field surrounding J1632–0033.

In the  $B$ -,  $V$ -, and  $R$ -band images, the optical counterpart of J1632–0033 is pointlike. The signal-to-noise ratio (peak/RMS) in these images was 13, 43, and 33, respectively. We therefore cannot rule out the presence of a second component that is dimmer by more than a factor of 4.3 in  $B$ , 14 in  $V$ , and 11 in  $R$  (using a  $3\sigma$  criterion). Because the radio flux density ratio is 12.4, these are not very strong constraints.

In the  $I$ -band image, which has a signal-to-noise ratio of 25, the counterpart does have a faint extension to the southeast at the  $3\sigma$  level. The lower left panel of Figure 3 shows a  $10'' \times 10''$  subraster from the  $I$ -band image. The lower right panel shows the surface brightness contours. The two black dots illustrate the relative separation of the radio components, as measured with the VLBA.

The separation and position angle of the dim extension are in rough agreement with the radio values. It may represent the optical counterpart to component B, and/or light from a lensing galaxy between components A and B. Based on the high radio flux density ratio between A and B, simple lens models would predict that the lensing galaxy should be situated very close to component B. The optical images are therefore consistent with both the binary quasar or gravitational lens hypotheses.

### 3.2. Optical spectrum

On 2000 September 1, we obtained an optical spectrum of J1632–0033 with the 3.5-meter telescope at Apache Point Observatory<sup>11</sup>. We used the Double Imaging Spectrograph in low resolution mode. The processed spectrum had a very weak signal, with two features at the  $1 - 2\sigma$  level whose wavelength ratio was consistent with the common quasar emission lines  $\text{Ly}\alpha$  ( $1216\text{\AA}$ ) and C IV ( $1549\text{\AA}$ ), allowing the tentative identification of J1632–0033 as a quasar at redshift 3.42.

This identification was confirmed on 2001 March 23, when we obtained an optical spectrum

---

<sup>11</sup>The Apache Point Observatory 3.5-meter telescope is owned and operated by the Astrophysical Research Consortium.

with the 6.5-meter Baade telescope at Las Campanas Observatory<sup>12</sup>. We used a Boller & Chivens slit spectrograph with a 600 lines mm<sup>-1</sup> grating, giving a pixel scale of 0".44 pixel<sup>-1</sup>, dispersion 2.75Å pixel<sup>-1</sup>, and wavelength coverage 4500–7300Å. We used the WG360 Schott glass blocking filter to block second order contamination. The slit was 1".3 wide, centered on component A, and oriented perpendicular to the A/B position angle.

Flat-fielding, spectrum extraction, and wavelength calibration were carried out with standard IRAF procedures. The processed spectrum is shown in Figure 4. Here the Ly $\alpha$  and C IV emission lines are detected with high significance, implying  $z = 3.424 \pm 0.007$ . The expected position of Si IV + O IV] (1400Å) is also shown.

#### 4. Discussion and summary

J1632–0033 consists of two radio components separated by 1".47. Both components are compact on milliarcsecond scales, although the brighter component is partially resolved. In measurements ranging from 1.4 GHz to 43 GHz, the spectral indices of the components are nearly the same. The brighter component, at least, is a spectroscopically verified quasar at redshift 3.42. What are the possible explanations for such a close pair of compact radio sources with the same radio “color”? Here we discuss the strengths and weaknesses of four hypotheses, in what we believe is the order of increasing likelihood: a chance alignment, a GPS quasar, a binary quasar, and a gravitational lens.

1. **Chance alignment.** In the 1.4 GHz NVSS catalog (Condon et al. 1998), there are  $\rho \approx 11$  sources deg<sup>-2</sup> brighter than 15 mJy in fields away from the galactic plane. The probability that two sources will be found within an angular radius of  $\Delta\theta = 1".5$  is:

$$P = 1 - \exp[-\rho\pi(\Delta\theta)^2] = 6 \times 10^{-6}. \quad (1)$$

The probability of finding one such alignment among a sample of 3850 radio sources is only about 2%.

If the spectral indices of the components are taken into account, the likelihood of a chance alignment drops by a factor of 60, as we now demonstrate. Figure 5 is the spectral index distribution  $f(\alpha)$  of 9966 radio sources, in bins of width  $\Delta\alpha = 0.05$ . This sample consists of all sources in the PMN tropical and equatorial catalogs with galactic latitude  $|b| > 10^\circ$  and flux density  $> 70$  mJy. The spectral indices were computed with reference to the NVSS catalog, as they were in our lens survey.

---

<sup>12</sup>The 6.5-meter Baade telescope is the first telescope of the Magellan Project, a collaboration between the Observatories of the Carnegie Institution of Washington, the University of Arizona, Harvard University, the University of Michigan, and MIT.

The mean sky density of sources within the  $i$ th bin is  $\rho \times f(\alpha_i)$ . Flat-spectrum sources ( $\alpha > -0.5$ ) constitute a fraction  $f_{\text{flat}} = 0.37$  of the total. Given the detection of one flat-spectrum source, the probability of a chance alignment with another flat-spectrum source that is within the same bin is

$$P' = \sum_{i=1}^N \frac{f(\alpha_i)}{f_{\text{flat}}} [1 - \exp(-\rho f(\alpha_i) \pi (\Delta\theta)^2)] = 10^{-7}. \quad (2)$$

Here the index  $i$  runs over all bins with  $\alpha_i > -0.5$ . Even with 3850 opportunities, the chance of finding another flat-spectrum source within  $1''.5$  with a spectral index that matches within 0.05 is only 0.04%. Sources fainter than 70 mJy may have a somewhat different spectral index distribution, but this would probably not change the order of magnitude of our calculation.

2. **GPS quasar.** As mentioned in the introduction, it is unusual for a radio source to have more than one component that is compact on milliarcsecond scales. This is the basis of our lens search strategy. Apart from lenses and binary quasars, there are only two categories of radio sources known to us that sometimes have two compact components: compact steep-spectrum (CSS) doubles and gigahertz-peaked-spectrum (GPS) sources (see O’Dea 1998 for a review).

As the name implies, CSS doubles have steep spectra (generally  $\alpha < -0.6$ ) and can be dismissed. However, it is apparent from the top panel of Figure 2 that the continuum radio spectrum of J1632–0033 may not be well-described by a power law throughout the whole range 1.4–43 GHz; it is flatter at the low end and steeper at the high end. Possibly this is a GPS quasar, with a peak between 1.4 GHz and 5 GHz.

The typical radio morphologies of GPS sources are miniature (sub-arcsecond) versions of those associated with classical radio galaxies: compact cores, core-jets, doubles, and linear triples. Nevertheless, J1632–0033 would be a most unusual GPS double, for four reasons:

- The optical counterparts of GPS quasars are generally unresolved points, whereas there appear to be two components in the optical counterpart of J1632–0033.
- The spectral slope of GPS sources at frequencies above the peak is usually steeper; O’Dea (1998) reports an average post-peak slope of  $\alpha = -0.77$ .
- The angular separation of GPS doubles is typically 10–100 mas, compared to the 1469 mas observed in J1632–0033.
- When the components of a GPS double exhibit extended structure, they are generally observed to extend towards one another, whereas the extension in component A (Figure 1) is nearly perpendicular to the direction to component B.

In the absence of a complete understanding of GPS sources and their distribution of their radio spectra, angular sizes, and morphologies, it is difficult to be quantitative about this hypothesis, but it seems very unlikely.

3. **Binary quasar.** Pairs of quasars at the same redshift, with physical separations of about 10–100 kiloparsecs, are at least 100 times more numerous than one would expect based on the correlation function of quasars on megaparsec scales. The leading explanation for this enhancement is mutually-induced nuclear activity in close pairs of galaxies (Djorgovski 1991; Kochanek, Falco & Muñoz 1999). The frequency of binary quasars among optically-selected samples of quasars is about  $2 \times 10^{-3}$ , which is coincidentally close to the frequency of lensing (Hewett et al. 1998; Kochanek, Falco & Muñoz 1999; Mortlock, Webster & Francis 1999). Binary quasars have therefore been a significant contaminant in lens searches based on optical imaging.

Binary quasars are less of a problem in radio lens surveys because radio-bright quasars constitute a minority of quasars generally. Only about 10% of optically-selected quasars are brighter than 10 mJy at 8.5 GHz (Hooper et al. 1996). This implies  $\sim 90\%$  of the binary quasars in our sample should have one member that is radio-faint. Assuming conservatively that all the flat-spectrum radio sources in our sample are quasars, and that the incidence of binaries is  $2 \times 10^{-3}$ , then the incidence of binaries in which both members are radio-bright is  $P = 2 \times 10^{-4}$ . There would be a 77% chance of finding one in our sample of 3850 sources.

However, when assessing whether J1632–0033 in particular is a binary quasar, the near-equality of the spectral indices of its components should be taken into account. The normalized spectral index distribution of flat-spectrum sources is  $f(\alpha)/f_{\text{flat}}$ , where  $f(\alpha)$  is the overall spectral index distribution discussed previously. The chance of randomly drawing two quasars with spectral indices within  $\Delta\alpha = 0.05$  is approximately

$$P = \sum_{i=1}^N \left[ \frac{f(\alpha_i)}{f_{\text{flat}}} \right]^2 = 0.05, \quad (3)$$

where, as before, the index  $i$  runs over all the bins with  $\alpha_i > -0.5$ . This reduces the likelihood of finding such a binary quasar in our sample to about  $77\% \times 0.05 = 4\%$ .

This calculation assumes that the radio continuum spectra of quasars in binary systems are not significantly correlated. This may be wrong, but at the moment this assumption is difficult to test. There is only one known example of a probable binary quasar in which both components are radio-bright (B0827+525; Koopmans et al. 2000), and it has spectral indices differing by  $\Delta\alpha = 0.25$ .

4. **Gravitational lens.** The incidence of gravitational lensing in our survey is expected to be at least  $P = 10^{-3}$ , both theoretically (Turner, Ostriker & Gott 1984) and empirically (judging from the lens discovery rate in CLASS, a large northern-hemisphere lens search; Myers 1999; Browne & Myers 2000). This is higher than the corresponding probabilities for a chance coincidence or binary quasar and leads us to expect at least 4 lenses in our survey; this is certainly consistent with J1632–0033 being the third lens discovered to date.

Furthermore, the near-equality of the radio continuum spectra of A and B is a natural consequence of the lensing hypothesis. Although the time delay can cause variations in the

instantaneous flux density ratio in gravitational lenses, if this ratio is observed to be constant it is good evidence for lensing.

There are two additional (weaker) indications in the data that J1632–0033 is a lens. First, the angular separation ( $\Delta\theta = 1''.47$ ) is more typical of lenses than binary quasars. The angular scale for lenses ( $0''.5$  to  $3''$ ) is set by the masses of the lens galaxies, which are typically  $L_*$  galaxies at  $z \sim 0.5$ . By contrast, binary quasars tend to have separations  $\Delta\theta > 3''$  (Mortlock, Webster & Francis 1999; Kochanek, Falco & Muñoz 1999). It has been suggested that small-separation binaries are rare because they represent a later, shorter-lived phase of the inspiral of merging galactic nuclei (Kochanek, Falco & Muñoz 1999). If this system is a binary quasar, it would have the second-smallest angular separation among the 20 probable binary quasars in the current literature (the smallest, by far, is  $0''.3$  in LBQS 0103–2753; Junkkarinen 2001).

Second, the VLBA image of component A (Figure 1, right panel) reveals a jet that is directed nearly perpendicular to the direction to component B. This is characteristic of the tangential stretching of gravitationally lensed images, whereas it would require a coincidence under the binary quasar hypothesis. Some examples of well-established lenses that exhibit tangential stretching in VLBI images are B0218+357 (Patnaik et al. 1995), B1422+231 (Patnaik et al. 1999), and MG 0414+0534 (Trotter, Winn & Hewitt 2000; Ros et al. 2000).

In summary, J1632–0033 is a strong candidate to be a strongly-lensed quasar. The separation, compactness, and spectral indices of the components do not fit well into any known category of radio sources besides gravitational lenses and binary quasars. The small separation and similar continuum radio spectra rule out a chance coincidence. The same evidence argues against the binary quasar hypothesis, which would anyway be intrinsically less probable than the lensing hypothesis because radio-bright quasars constitute a minority of all quasars.

Here we suggest two lines of observational inquiry that would settle the matter. Deeper and higher-resolution VLBI imaging may resolve component B; this might reveal parity-reversed substructure corresponding to the jet observed in A, and would be additional circumstantial evidence for lensing. However, the highest priority should be optical imaging. Deeper and higher resolution images than those presented in § 3.1 will test for the presence of a foreground galaxy. In many other cases this has required the *Hubble Space Telescope*. This particular case is favorable for adaptive-optics imaging, because there is a bright ( $R = 12.2$ ) star located  $27''.5$  south (see Figure 3) that is available as a guide star.

We are grateful to Ed Turner, for arranging the APO spectroscopic observations; to Phillip Helbig and David Rusin, for making available the archival VLA data from June 1999; to Chris Fassnacht, for his assistance with the VLBA; and to Tom Muxlow and Peter Thomasson, for their assistance with MERLIN. This research was supported by the National Science Foundation under grants AST-9617028 and AST-9616866. J.N.W. thanks the Fannie and John Hertz foundation for financial support.

## REFERENCES

- Blandford, R.D. & Narayan, R. 1992, *ARA&A*, 30, 311
- Browne, I.W.A. & Myers, S. 2000, to appear in *New Cosmological Data and the Values of the Fundamental Parameters*, Proc. IAU Symposium 201, Manchester, England
- Condon, J.J., Cotton, W.D., Greisen, E.W., Yin, Q.F., Perley, R.A., Taylor, G.B., & Broderick, J.J. 1998, *AJ*, 115, 1693
- Djorgovski, G. 1991, ASP Conf. 21, *Space Distribution of Quasars*, ed. D. Crampton (San Francisco: ASP), 349
- Falco, E.E., Impey, C.D., Kochanek, C.S., Lehár, J., McLeod, B.A., Rix, H.-W., Keeton, C.R., Muñoz, J.A., & Peng, C.Y. 1999, *ApJ*, 523, 617
- Fukugita, M., Futamase, T., & Kasai, M. 1990, *MNRAS*, 246, 24
- Garrett M.A., Porcas, R.W., Nair, S., & Patnaik, A.R. 1997, *MNRAS*, 279, L7
- Griffith, Mark R., Wright, Alan E., Burke, B.F., & Ekers, R.D. 1995, *ApJS*, 97, 347
- Griffith, Mark R. & Wright, Alan E. 1993, *AJ*, 105, 1666
- Hewett, Paul C., Foltz, Craig B., Harding, Margaret E., & Lewis, Geraint F. 1998, *AJ*, 115, 383
- Hooper, E.J., Impey, C.D., Foltz, C.B., & Hewett, P.C. 1996, *ApJ*, 473, 746
- Junkkarinen, V., Shields, G.A., Beaver, E.A., Burbidge, E.M., Cohen, R.D., Hamann, F., & Lyons, R.W. 2001, preprint (astro-ph/0102501)
- King, Lindsay J., Browne, Ian W.A., Marlow, Daniel R., Patnaik, Alok R., & Wilkinson, Peter N. 1998, *MNRAS*, 307, 225
- Kochanek, C.S. 1995, *ApJ*, 445, 559
- Kochanek, C.S., Falco, E.E., & Muñoz, J.A. 1999, *ApJ*, 510, 590
- Koopmans, L.V.E., de Bruyn, A.G., Fassnacht, C.D., Marlow, D.R., Rusin, D., Blandford, R.D., Browne, I.W.A., Helbig, P., Jackson, N., Myers, S.T., Pearson, T.J., Readhead, A.C.S., Wilkinson, P.N., Xanthopoulos, E., & Hoekstra, H. 2000, *A&A*, 361, 815
- Landolt, A.U. 1992, *AJ*, 104, 340
- Lawrence, C.R., Bennett, C.L., Hewitt, J.N., Langston, G.I., Klotz, S.E., Burke, B.F., & Turner, K.C. 1986, *ApJS*, 61, 105
- Mortlock, D.J., Webster, R.L., & Francis, P.J. 1999, *MNRAS*, 309, 836

- Myers, S. 1999, PNAS, 96, 4236
- Narayan R. 1998, New Astronomy Reviews, 42, 73
- O’Dea, C.P. 1998, PASP, 110, 493
- Patnaik, A.R., Porcas, R.W., & Browne, I.W.A. 1995, MNRAS, 274, L5
- Patnaik, A.R., Kembell, A.J., Porcas, R.W., & Garrett, M.A. 1999, MNRAS, 307, L1
- Refsdal, S. MNRAS, 128, 307
- Ros, E., Guirado, J.C., Marcaide, J.M., Pérez-Torres, M.A., Falco, E.E., Muñoz, J.A., Alberdi, A., & Lara, L. 2000, A&A, 362, 845
- Tasker, Niven J., Condon, J.J., Wright, Alan E., & Griffith, Mark R. 1994, AJ, 107, 2115
- Trotter, Catherine S., Winn, Joshua N., & Hewitt, Jacqueline N. 2000, ApJ, 535, 671
- Turner, E. 1990, ApJ, 365L, 43
- Turner, E.L., Ostriker, J.P., & Gott, J.R., III 1984, ApJ, 284, 1
- Winn, J.N., Hewitt, J.N., Schechter, P.L., Dressler, A.D., Falco, E.E., Impey, C.D., Kochanek, C.S., Lehar, J., Lovell, J.E.J., McLeod, B.A., Morgan, N.D., Muñoz, J.A., Rix, H.-W., & Ruiz, M.T. 2000, AJ, 120, 2868
- Winn, Joshua N., Hewitt, Jacqueline N., Patnaik, Alok R., Schechter, Paul L., Schommer, Robert A., López, Sebastian, Maza, José, & Wachter, Stefanie 2001, AJ, 121, 1223

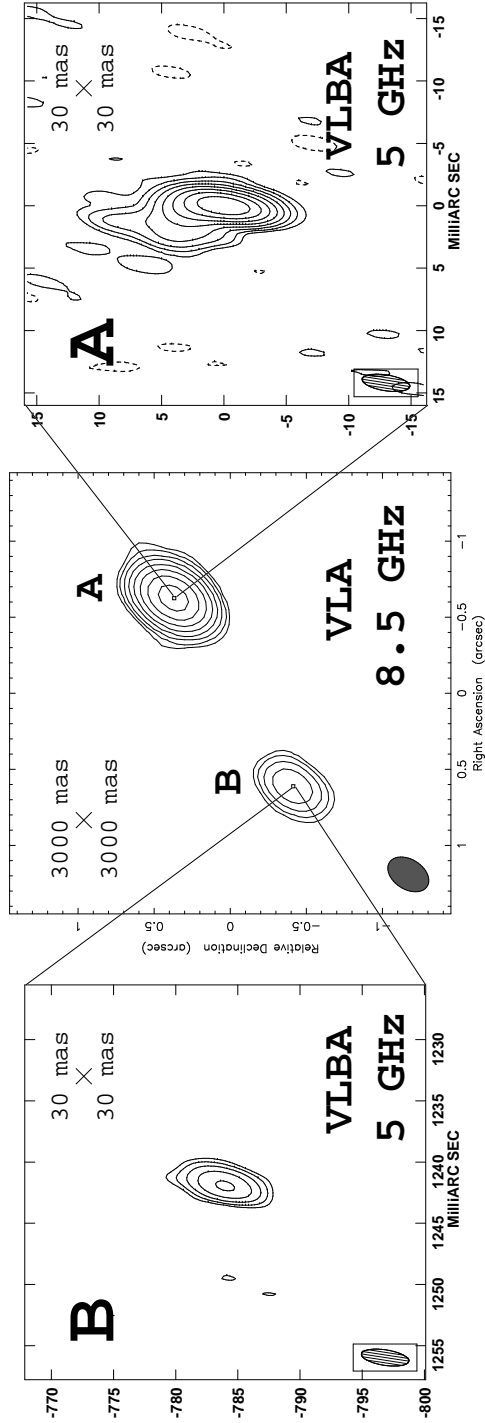


Fig. 1.— Radio images of J1632–0033. The central panel derives from the 8.5 GHz VLA observation of 1994 February 24. The left and right panels are close-ups of each radio component, from the 5 GHz VLBA data of 2000 April 29. All images are based on uniform weighting of the visibility data. Contours begin at  $3\sigma$  and increase by powers of 2, where  $\sigma$  is the RMS level in the residual map. The restoring beam is inset in the lower left of each map.

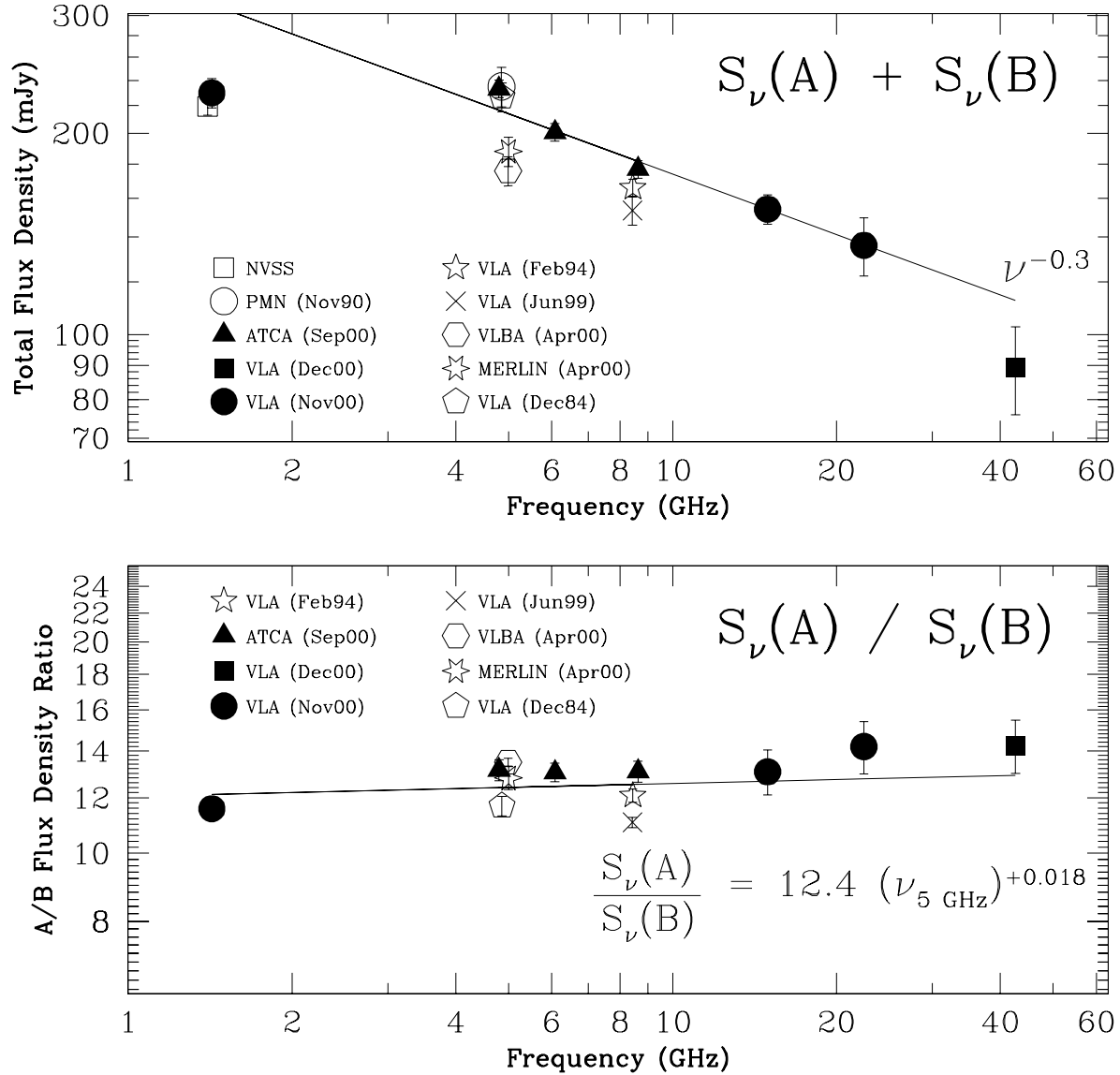


Fig. 2.— **Top panel.** Total flux density of J1632–0033 as a function of radio frequency. All the measurements in Table 1 are plotted, as are the entries from the PMN (Griffith et al. 1995) and NVSS (Condon et al. 1998) catalogs. The measurements span a 16-year period; however, the filled symbols all represent measurements made between September and December 2000. For reference, a power law  $S_\nu \propto \nu^{-0.3}$  (chosen to match the points from 5 GHz to 22.5 GHz) is also plotted.

**Bottom panel.** Flux density ratio as a function of radio frequency. The error estimates were computed by assuming that the uncertainty in the relative flux density scale is equal to the RMS noise level in the image. The solid line is based on a linear least-squares fit to the data points.

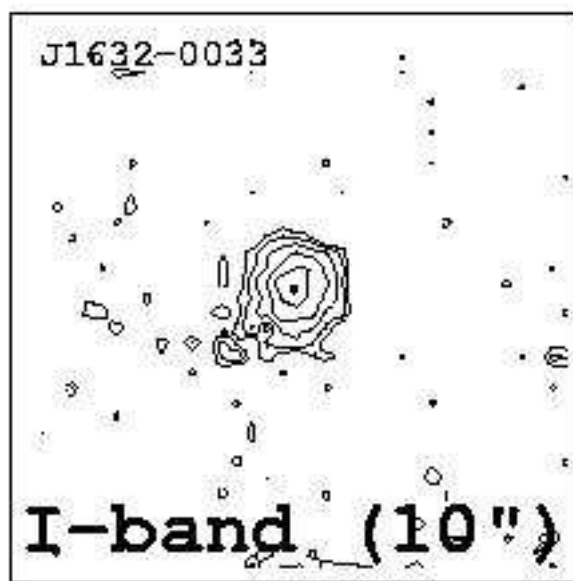
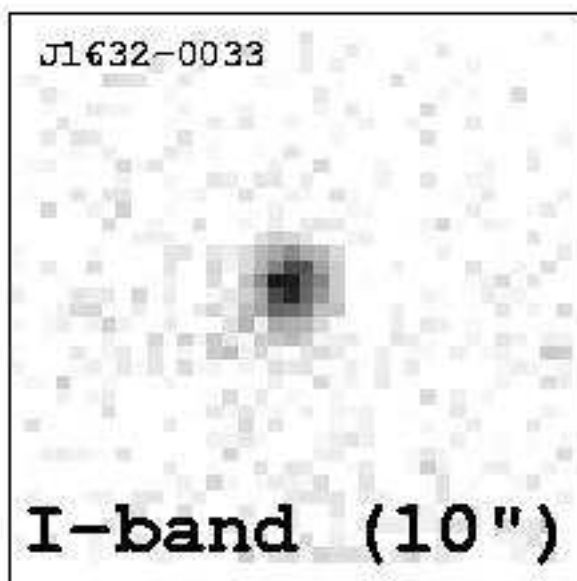
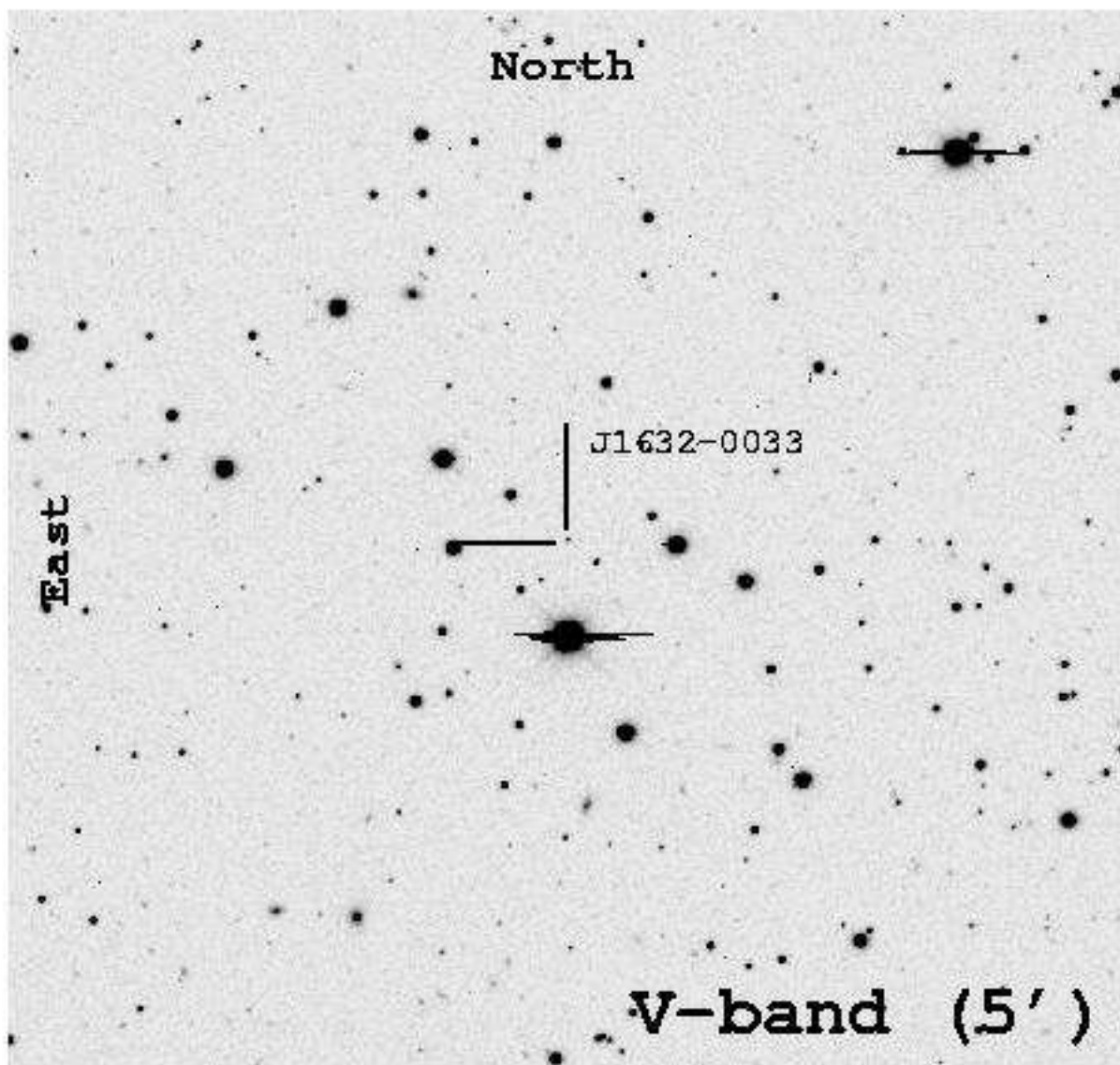


Fig. 3.— **Top panel.** Optical field surrounding J1632-0033. This  $5' \times 5'$  field is derived from the V-band image described in § 3.1. The cross-hairs identifying J1632-0033 are  $30''$  long.

**Bottom left panel.** A subraster ( $10'' \times 10''$ ) of the I-band image, centered on J1632-0033.

**Bottom right panel.** Contour plot of the same I-band subraster. The contour levels begin at  $2\sigma$  and increase by factors of 1.5. Two black dots have been added to the figure with the same relative separation as the radio components.

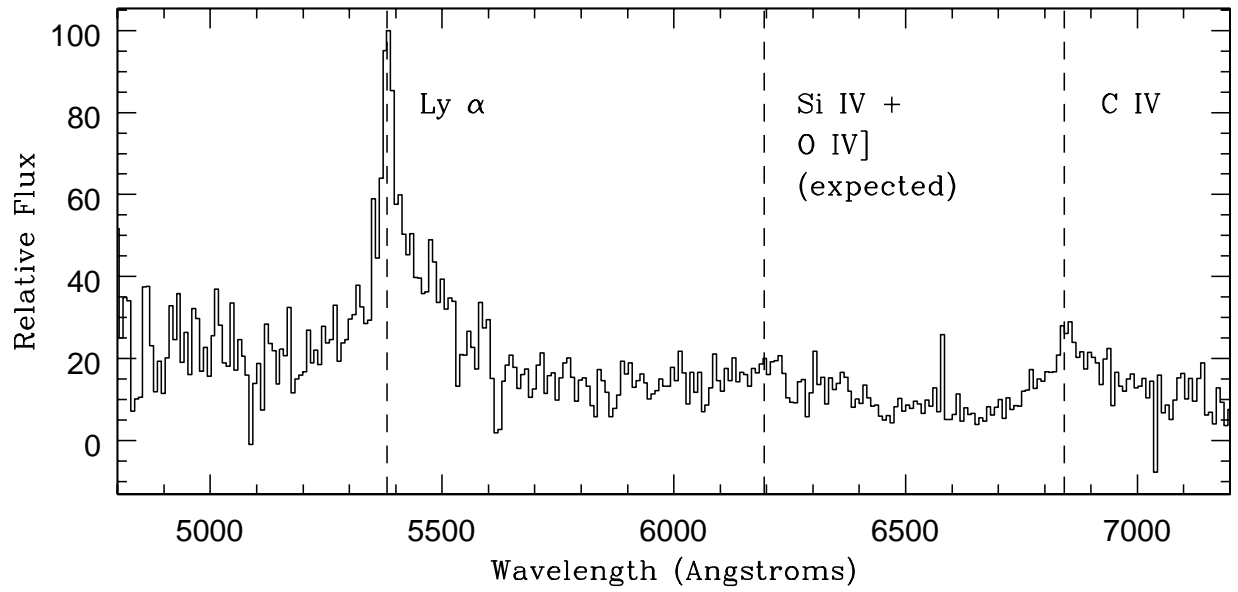


Fig. 4.— Optical spectrum of component A of J1632–0033 (see § 3.2).

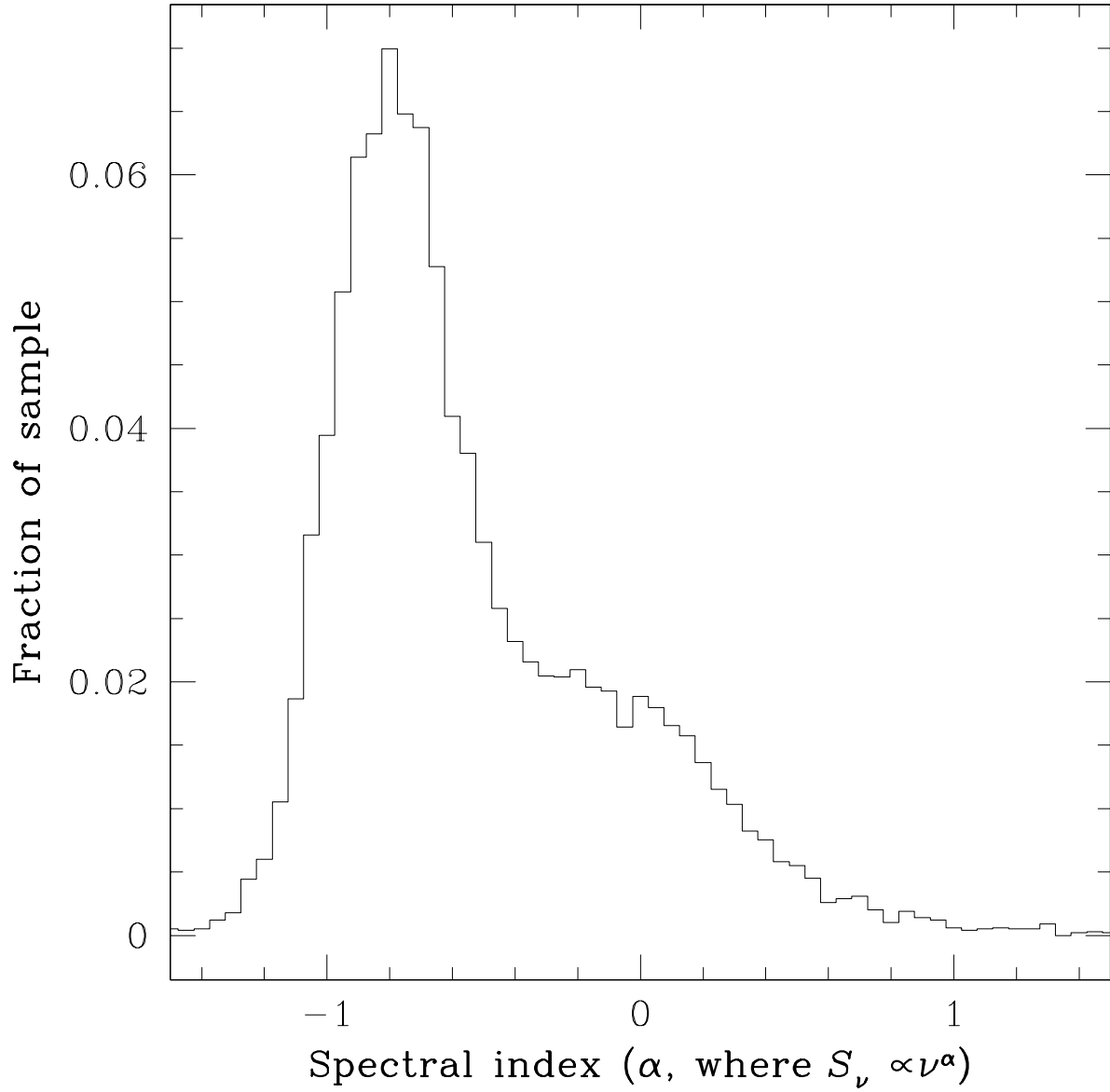


Fig. 5.— Histogram of spectral indices in a sample of 9966 radio sources from the 4.85 GHz PMN tropical and equatorial radio catalogs. The selection criteria for the sample were: (a) flux density  $> 70$  mJy; (b)  $|b| > 10^\circ$ . Spectral indices were computed between the PMN flux and the sum of the fluxes of all sources within  $100''$  in the 1.4 GHz NVSS catalog.

Table 1. Radio observations of J1632–0033

Date	Observatory	Frequency (GHz)	Bandwidth (MHz)	Duration (min)	Beam FWHM (mas $\times$ mas, P.A.)	Flux density		RMS noise (mJy beam <sup>-1</sup> )	Abs. flux uncertainty
						A (mJy)	B (mJy)		
1984 Dec 17	VLA	4.860	100	1.3	435 $\times$ 332 (6°)	208.77	17.87	0.57	5%
1994 Feb 24	VLA	8.452	50	1.3	294 $\times$ 196 (–33°)	153.13	12.67	0.27	3%
1999 Jun 30	VLA	8.440	100	1.5	743 $\times$ 207 (54°)	140.66	12.71	0.22	5%
2000 Apr 05	MERLIN	4.994	15	110	95.2 $\times$ 42.6 (22°)	174.28	13.61	0.51	5%
2000 Apr 29	VLBA	4.987	32	54	3.41 $\times$ 1.41 (–2°)	163.59	12.13	0.15	5%
2000 Sep 26	ATCA	4.800	128	5	1385 $\times$ 9840 (0°)	216.62	16.48	0.57	3%
2000 Sep 26	ATCA	6.080	128	10	1140 $\times$ 2600 (0°)	186.44	14.29	0.43	3%
2000 Sep 26	ATCA	8.640	128	15	791 $\times$ 2020 (0°)	164.18	12.56	0.43	3%
2000 Nov 11	VLA	1.425	100	2.0	3370 $\times$ 1140 (53°)	211.63	18.28	0.33	5%
2000 Nov 11	VLA	14.940	100	0.5	242 $\times$ 115 (52°)	143.09	10.95	0.80	5%
2000 Nov 11	VLA	22.460	100	5.9	184 $\times$ 79.8 (53°)	127.03	8.95	0.76	10%
2000 Dec 24	VLA	42.640	100	12	62.1 $\times$ 39.7 (–46°)	83.43	5.86	0.51	15%

Note. — The J2000 coordinates of component A are R.A. = 16<sup>h</sup>32<sup>m</sup>57<sup>s</sup>.680, Decl. = –00°33′21″.05, within 0″.15. The separation between A and B is  $\Delta$ R.A. = 1242.4  $\pm$  1.7 mas,  $\Delta$ Decl. = 783.3  $\pm$  0.7 mas, based on the 5 GHz VLBA data of 2000 April 29.

Table 2. Optical observations of J1632–0033

Filter	Duration (seconds)	Seeing (arcsec)	Airmass	Total magnitude
<i>I</i>	600	1.07	1.23	$20.25 \pm 0.05$
<i>I</i>	600	1.15	1.20	$20.25 \pm 0.05$
<i>B</i>	600	1.15	1.18	$23.02 \pm 0.08$
<i>V</i>	600	1.00	1.17	$21.33 \pm 0.05$
<i>R</i>	600	1.24	1.16	$20.88 \pm 0.05$